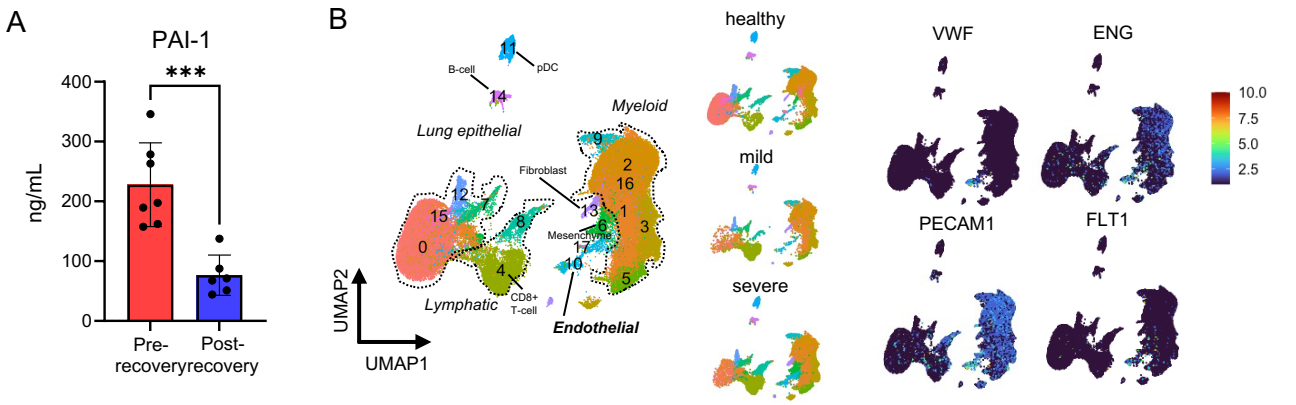

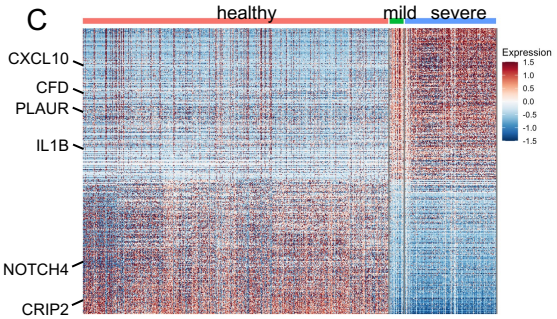

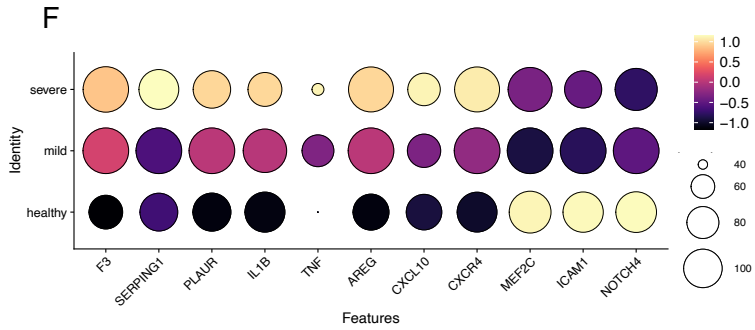

D

Upregulated in patient EC (healthy V.S. severe)

Term name	adjusted P value
TYROBP Causal Network	1.18.E-13
Microglia Pathogen Phagocytosis Pathway	2.19.E-10
Allograft Rejection	9.72.E-07
Macrophage markers	1.27.E-06
Ebola Virus Pathway on Host	1.46.E-04
Complement and Coagulation Cascades	7.60.E-04
Human Complement System	1.62.E-03
COVID-19 Adverse Outcome Pathway	1.85.E-03
Iron metabolism in placenta	1.46.E-02
Viral Acute Myocarditis	1.82.E-02
Cytokines and Inflammatory Response	3.32.E-02

Downregulated in patient EC (healthy V.S. severe)

Term name	adjusted P value
Ebola Virus Pathway on Host	6.93.E-04
VEGFA-VEGFR2 Signaling Pathway	2.31.E-03
Spinal Cord Injury	9.37.E-03
Adipogenesis	2.26.E-02
Leptin Insulin Overlap	3.42.E-02
Glucocorticoid Receptor Pathway	4.89.E-02

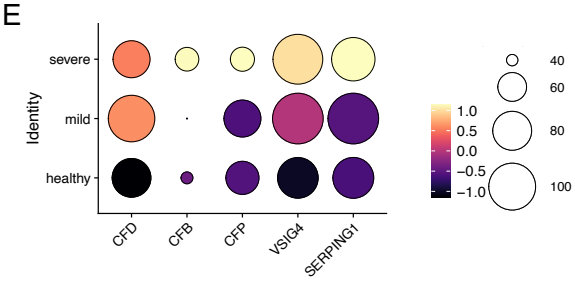

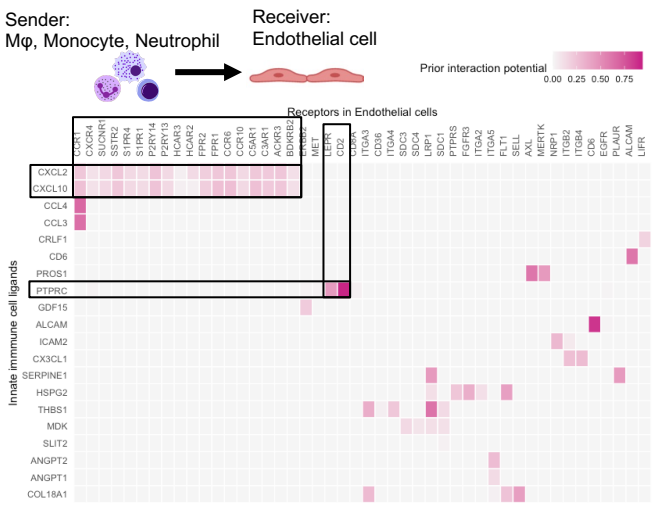

Supplementary Figure 1. Endotheliopathy signatures in the COVID-19 recovered patient serum and patient single cell transcriptomics. Related to Figure 1 (**A**) Quantification of PAI-1 in non-ICU COVID-19 patient (Caucasian/Non-Hispanic) plasma pre- and post- recovery, which were collected at a different institution (mean ± SD; n=7 per group; ***p < 0.001 evaluated by Welch's t-test). (**B**) Uniform manifold approximation and projection (UMAP) plot of public BALF single cell RNA-seq data colored by cell type (left; patient group integrated, center; split by patient group). The feature plots showing the expression of endothelial cell type markers (right). (**C**) Heatmap showing a set of genes with altered expression in endothelial cell from infected patients. (**D**) List of pathways significantly positively or negatively enriched in endothelial cells in severe patient group. (**E**) Dot plot representing gene expression of complement pathway genes that changed significantly among each endothelial cell group. The size of dots indicates the relative gene expression in percent for each group. The color represents the average expression level for the indicated gene. (**F**) Dot plot representing gene expression of inflammation associated genes that changed significantly among each endothelial cell group. (**G**) Heatmap showing the predicted ligand-receptor interactions between sender; innate immune cells (macrophages (Mφ), monocyte, and neutrophil) and receiver; endothelial cells in severe patient.

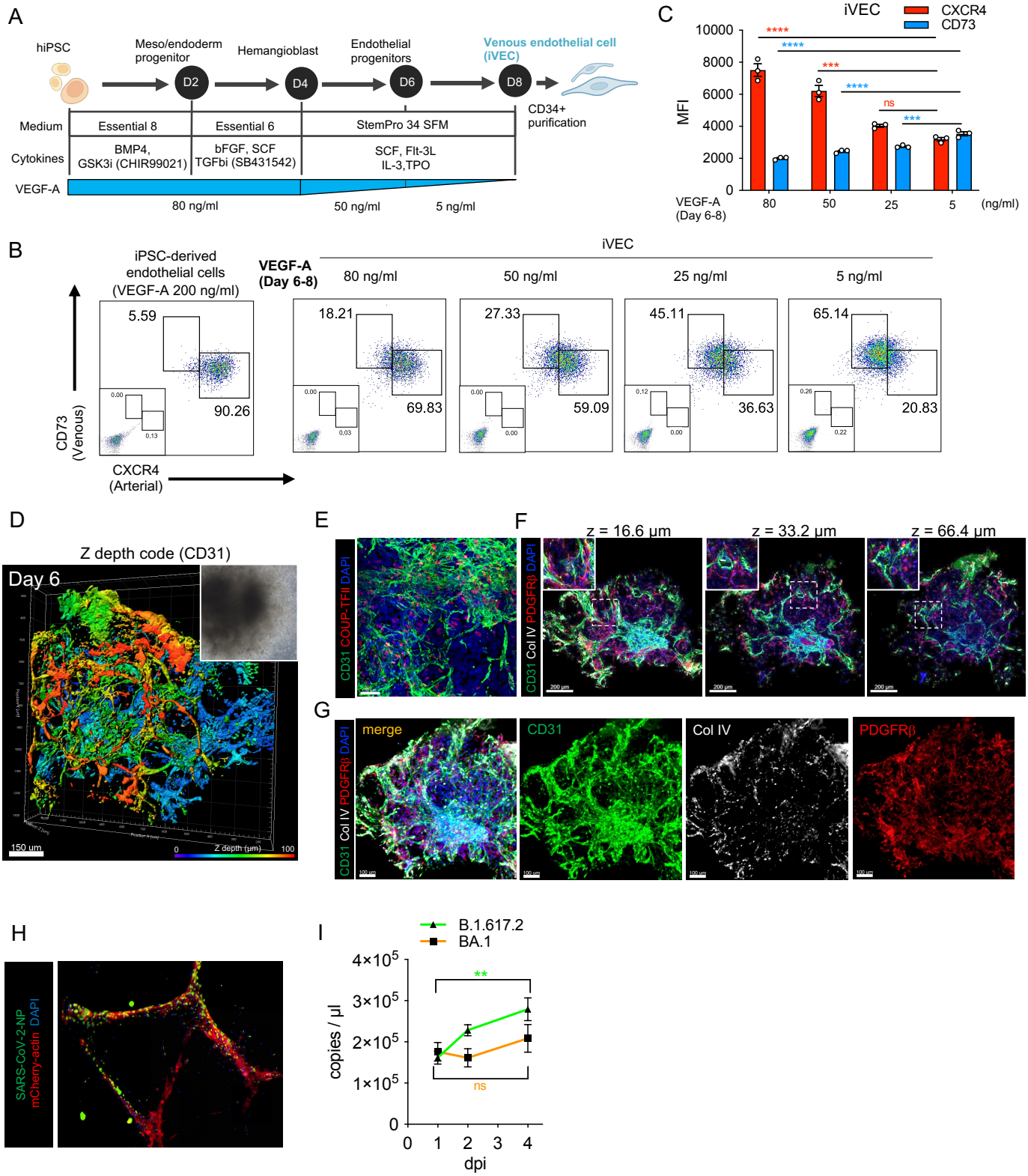

Supplementary Figure 2. Induction and characterization of SARS-CoV-2 infection-competent iVO derived from venous endothelium. Related to Figure 2. (A) The schema of iPSC-derived venous endothelial cell (iVEC) differentiation **(B)** Scatter dot-plot of the flow cytometry analysis of CD73/CXCR4 expression at day 8 by different concentrations of VEGF-A at day 6-8. **(C)** Quantification of CD73 and CXCR4 mean fluorescent intensity (MFI) (n=3; mean ± SE; One-Way ANOVA with Dunnet's post-hoc test compared to 5 ng/ml VEGF-A condition; ***$p < 0.001$; ****$p < 0.0001$). **(D)** Whole-mount 3D reconstructed image of iVO with immunofluorescent staining for CD31 at day 6, and bright field image of iVO (upper right). **(E)** Whole-mount images of branched endothelial network in iVO with immunofluorescent staining for CD31 and COUP-TFII. **(F)** Cross-sectional view of whole-mount image of iVO with immunofluorescent staining for CD31, PDGFRb, and collagen IV. **(G)** Whole mount merged and single fluorescent channel images of iVO with immunofluorescent staining for CD31 and PDGFRb, and collagen IV. **(H)** Immunofluorescent staining of iVO for SARS-CoV-2 NP/mCherry-actin/DAPI at 4 dpi. **(I)** Time-series fold change in SARS-CoV-2 viral copy number in cell culture supernatant expression of iVOs infected with B.1.617.2 or BA.1 (n=4; mean ± SE; Two-Way ANOVA; **$p < 0.01$).

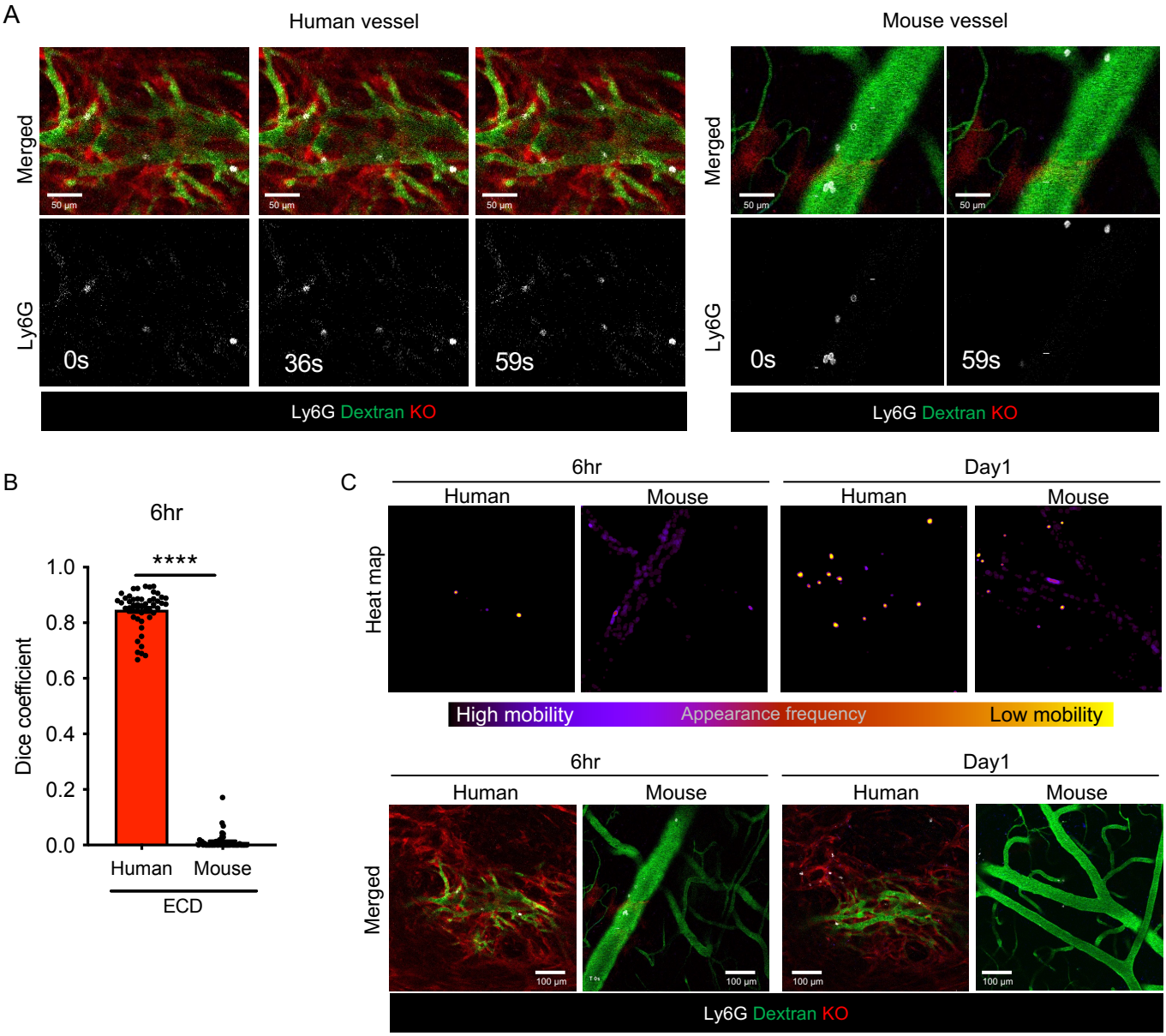

Supplementary Figure 3. Tracking analysis of neutrophils in human and mouse vessels after spike-ECD treatment. Related to Figure 3 (A) Intravital time-lapse imaging of neutrophils within human (transplant; left) and mouse (right) blood vessels 6 hrs after spike-ECD infusion. (**B**) Evaluation of the spatial overlap of neutrophils between the frames from time-lapse movie by the Dice coefficient 6 hrs after spike-ECD treatment. Representative time-lapse movies from three independent experiments of each group were quantified and neutrophils are displayed as dots. Data shown as mean ± SE; ****p<0.0001 evaluated by Welch's t-test. (**C**) Upper, Heatmap visualization of neutrophil mobility after spike-ECD treatment. Lower, representative intra-vital imaging of neutrophil in human and mouse vessels after spike-ECD treatment.

A

Upregulated in Late recovery (Day 1-2)

Term name	adjusted P value
Complement and coagulation cascades	1.91E-10
Complement activation	3.96E-06

Upregulated in Early recovery (Day 1-2)

Term name	adjusted P value
Pathogenic Escherichia coli infection	2.64E-03
Parkin-ubiquitin proteasomal system pathway	5.69E-03

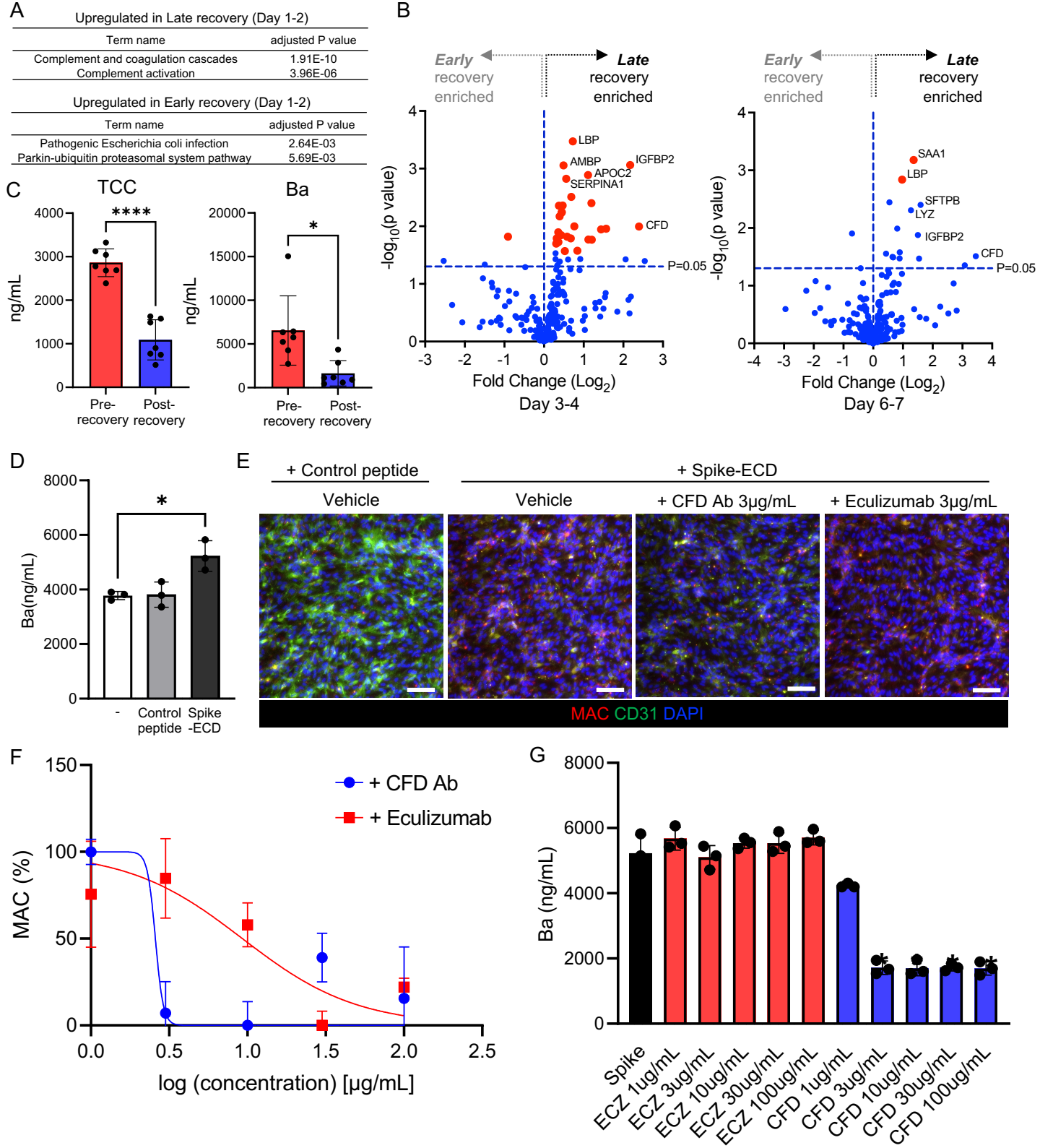

Supplementary Figure 4. Proteome analysis in patient plasma and potency of acid-switch half-life extension factor D targeting antibody. Related to Figure 4 and 5. (A) List of pathways significantly positively enriched in late recovery group at day1-2. (**B**) Volcano plots showing longitudinal differentially expressed protein profile between late recovery and early recovery at day 3-4 (left) and day 6-7 (right) post ICU admission. (**C**) Quantification of TCC (left) and Ba (right) in non-ICU COVID-19 patient (Caucasian/Non-Hispanic) plasma pre- and post- recovery, which were collected at a different institution (mean ± SD; n=7 per group; *p < 0.05; ****p<0.0001; Welch's t-test). (**D**) The level of complement factor Ba 24hrs after treatment with SARS-CoV-2 spike-ECD in culture supernatant of iPSC endothelial cells (mean ± SD; n=3 per group; *p<0.01 compared to control by ANOVA followed by Dunnett's test). (**E**) Immunostaining images demonstrated inhibition of MAC deposition on iPSC endothelial cells induced by spike-ECD under treatment of anti-CFD and anti-C5 (Eculizumab), Scale bars, 100 μm. (**F**) Quantification of dose dependent inhibition of MAC deposition. (**G**) Complement factor Ba levels in culture supernatant of iPSC derived endothelial cells treated simultaneously with anti-factor D and anti-C5 (eculizumab) (mean ± SD; n=3 per group; *p<0.05; compared to spike-ECD by ANOVA with Dunnett's post-hoc test).

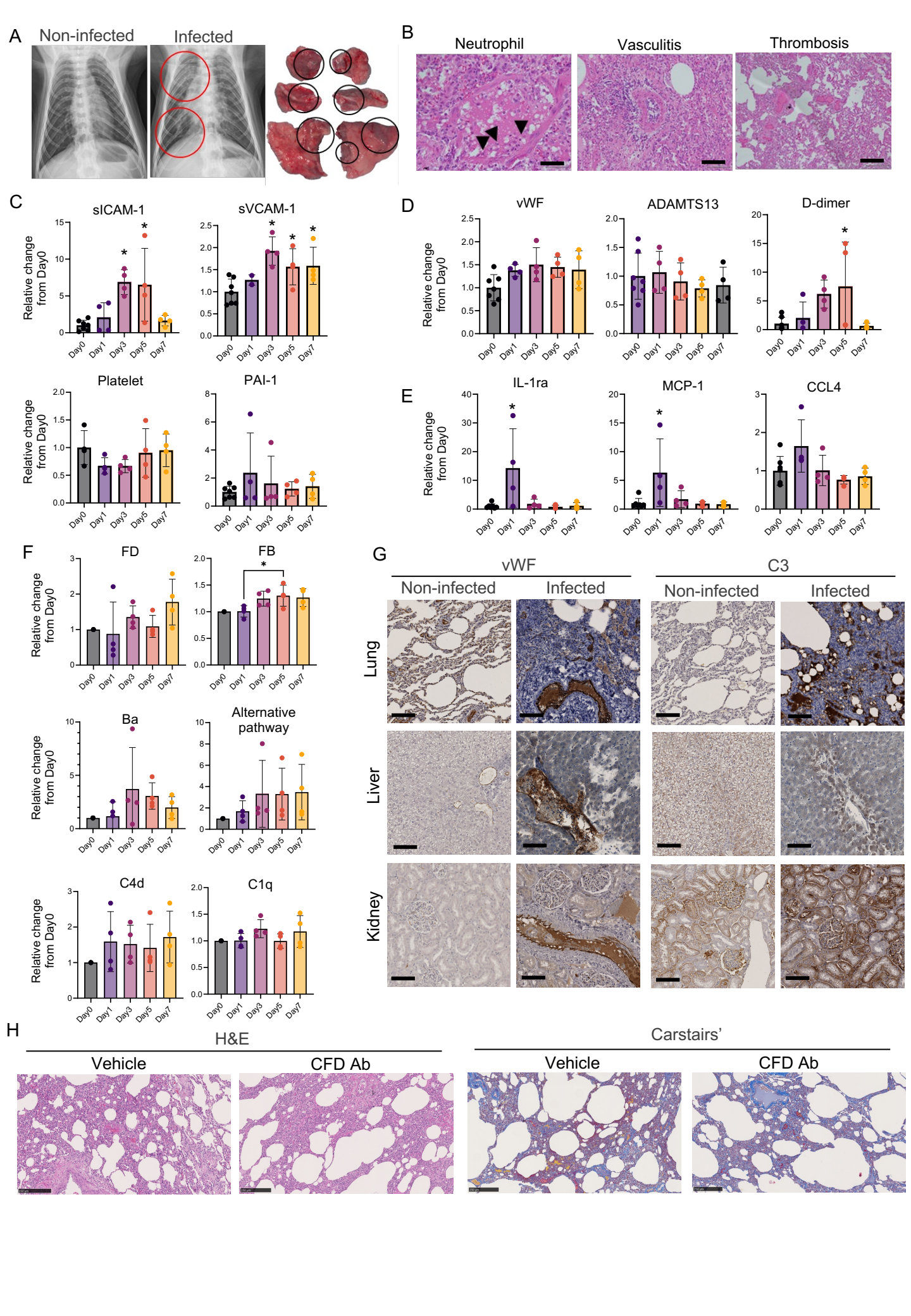
A
Non-infected
Infected
B
Neutrophil
Vasculitis
Thrombosis
C
sICAM-1
sVCAM-1
Platelet
PAI-1
Relative change from Day0
Day0
Day1
Day3
Day5
Day7
D
vWF
ADAMTS13
D-dimer
E
IL-1ra
MCP-1
CCL4
F
FD
FB
Ba
Alternative pathway
C4d
C1q
G
vWF
C3
Non-infected
Infected
Lung
Liver
Kidney
H
H&E
Carstairs'
Vehicle
CFD Ab

Supplementary Figure 5. Non-human primate COVID-19 model develops inflammathrombotic phenotype. Related to Figure 5 (A) Left, representative X-ray radiograph of cynomolgus macaques (CMs) before SARS-CoV-2 infection and 3 days after infection. Red circles indicate pulmonary infiltrates and opacity. Right, lung macroscopic appearance of autopsied macaques 3 days after virus inoculation. Black circles indicate lung lesions. (**B**) Hematoxylin-eosin staining of macaque lung tissue 3 days after infection with SARS-CoV-2. Scale bars, 100 μm. (**C**) The level of sICAM-1, sVCAM-1, PAI-1 in plasma collected on the indicated days. The count of platelet in peripheral blood cells (mean ± SD; n=4 or 7 per group; *p<0.05 compared to control by ANOVA followed by Dunnett's test). (**D**) vWF, ADAMTS13, D-dimer in plasma collected on the indicated days (mean ± SD; n=4 or 7 per group; *p<0.05 compared to control by ANOVA followed by Dunnett's test). (**E**) Inflammatory cytokines and chemokines (IL-1ra, MCP-1, CCL4) in plasma collected on the indicated days (mean ± SD; n=4 or 7 per group; *p<0.05 compared to control by ANOVA followed by Dunnett's test). (**F**) The level of factor D, factor B, factor Ba and C1q in plasma collected on the indicated days and analyzed by multi-plex assay. The activity of alternative pathway in serum and C4d expression in plasma measured by ELISA (mean ± SD; n=4 per group; *p<0.05 compared to control by ANOVA followed by Tukey's post-hoc test). (**G**) Immunohistochemistry (IHC) of C3 and vWF on lung, liver, and kidney of uninfected and infected macaques 7 days after SARS-CoV-2 inoculation. Scale bars, 100 μm. (**H**) Hematoxylin-eosin staining and Carstairs' staining of macaque lung tissue 3 days after infection with SARS-CoV-2 and anti-CFD. Scale bars, 250 μm.